UC Santa Barbara

UC Santa Barbara Previously Published Works

Title

Linking tree physiological constraints with predictions of carbon and water fluxes at an old-growth coniferous forest

Permalink

https://escholarship.org/uc/item/26x7d9g6

Journal

Ecosphere, 10(4)

ISSN

2150-8925

Authors

Jiang, Yueyang
Kim, John B
Trugman, Anna T
et al.

Publication Date

2019-04-01

DOI

10.1002/ecs2.2692

Peer reviewed

eScholarship.org Powered by the California Digital Library
University of California

esa

ECOSPHERE

Linking tree physiological constraints with predictions of carbon and water fluxes at an old-growth coniferous forest

YUEYANG JIANG [1,†] JOHN B. KIM [2] ANNA T. TRUGMAN [3] YOUNGIL KIM [1] AND CHRISTOPHER J. STILL [1]

[1]*Department of Forest Ecosystems & Society, Oregon State University, Corvallis, Oregon, USA*
[2]*USDA Forest Service, Pacific Northwest Research Station, Corvallis, Oregon, USA*
[3]*School of Biological Sciences, University of Utah, Salt Lake City, Utah, USA*

Citation: Jiang, Y., J. B. Kim, A. T. Trugman, Y. Kim, and C. J. Still. 2019. Linking tree physiological constraints with predictions of carbon and water fluxes at an old-growth coniferous forest. Ecosphere 10(4):e02692. 10.1002/ecs2.2692

Abstract. Old-growth coniferous forests of the Pacific Northwest are among the most productive temperate ecosystems and have the capacity to store large amounts of carbon for multiple centuries. To date, there are considerable gaps in modeling ecosystem fluxes and their responses to physiological constraints in these old-growth forests. These model shortcomings limit our ability to understand and project how the old-growth forests of the Pacific Northwest will respond to global climate change. This study applies the cohort-based Ecosystem Demography Model 2 (ED2) to the Wind River Experimental Forest (Washington, USA), a well-studied old-growth Douglas-fir–western hemlock ecosystem. ED2 is calibrated and validated using an extensive suite of forest inventory, eddy covariance, and biophysical observations. ED2 is able to reproduce observed forest composition and canopy structure, and carbon, water, and energy fluxes at the site. In the simulations, the effect of limited water supply on ecosystem carbon fluxes is mediated primarily by the forest's gross primary productivity (GPP) response, rather than its heterotrophic respiration response. The simulation indicates that stomatal conductance is mainly determined by soil moisture during periods of low vapor pressure deficit (VPD). However, when VPD is high, stomatal conductance is greatly reduced regardless of soil moisture status. During summer droughts, reduced soil moisture and increased VPD result in considerable stomatal closure and GPP reduction, which in turn decreases net carbon uptake. Cohort-based scheme integrates all canopy layers (species) that have distinct sensitivity to microclimate and respond distinctly to drought. This study is an initial first step to explore the potential importance of cohort-based model in simulating forest with complex structure, and to lay the foundation for applying cohort-based model at regional scales across the Pacific Northwest.

Key words: carbon flux; cohort-based model; old-growth coniferous forest; physiological constraint; tree physiology; water flux.

Received 13 November 2018; revised 13 February 2019; accepted 21 February 2019. Corresponding Editor: Yude Pan.
Copyright: © 2019 The Authors. This is an open access article under the terms of the Creative Commons Attribution License, which permits use, distribution and reproduction in any medium, provided the original work is properly cited.
† **E-mail:** yueyang.jiang@oregonstate.edu

INTRODUCTION

Old-growth coniferous forests, formerly widespread in the U.S. Pacific Northwest, have unique leaf physiological and conifer forest structural characteristics (White et al. 2000, Hessl et al. 2004). They are typically dominated by tall evergreen conifer species, such as Douglas-fir (*Pseudotsuga menziesii* (Mirb.) Franco), which can live for 400–1000 yr (Franklin and DeBell 1988, Falk et al. 2005), and western hemlock (*Tsuga heterophylla* (Raf.) Sarg.). These forests potentially store more aboveground carbon than any other forest type in the world (Franklin and Waring 1980, Schimel et al. 2000, Smithwick et al. 2002, Suchanek et al. 2004, Hudiburg et al. 2009) and are extremely heterogeneous in canopy structure, tree size, and understory patchiness (Franklin et al. 1981). As one of the most productive temperate forest ecosystems (Franklin and Waring 1980,

Field and Kaduk 2004), old-growth coniferous forests have the capacity to both assimilate large amounts of carbon (Paw U et al. 2004) and store carbon for multiple centuries in live, woody debris, and soil carbon pools (Harmon et al. 2004). Estimates of late-successional and old-growth forests in the Northwest Forest Plan area (western Oregon and Washington, and northern California) put the estimate at 3.0 Mha, with less than a 3% decrease on federal lands by 2012 (Davis et al. 2015). Under a projected warming climate, more frequent drought- and heat-related physiological stresses can substantially affect carbon and water cycling of the old-growth forests and the feedback to atmosphere (Law and Waring 2015). Given the importance of these forests to regional carbon and water budgets and the provision of ecosystem services, along with their societal value, it is imperative to understand the mechanisms that control carbon and water dynamics and responses to environmental changes.

Given the structural complexities of the old-growth forest (Franklin et al. 2002), species composition and size distribution may be important factors in shaping carbon and water dynamics between the ecosystem and atmosphere. The highly decoupled microclimate across different canopies drives distinct responses to physiological stresses among species/sizes. As climate warms in the region, potentially stronger water stress and higher mortality rates may alter forest composition (Littell et al. 2010, Spies et al. 2010), drive long-term change in forest productivity (Latta et al. 2010), and raise new challenges for future conservation planning (Carroll et al. 2010, Kim et al. 2017). Moreover, potential drought-related increase in future wildfire activities may dramatically change the forest structure in the region and release large amounts of carbon to the atmosphere (Abatzoglou and Williams 2016, Riley and Loehman 2016). The ongoing transition to more shade-tolerant species—the replacement of Douglas-fir with western hemlock (Bible 2001)—may change the ecosystem-level water-use efficiency and carbon assimilation rate in the region. Therefore, models that can reproduce species composition, canopy structure, and competitions among species/sizes are best equipped to evaluate the forest responses to climate change.

To date, several terrestrial biome models have been applied to the evergreen coniferous forests in the Pacific Northwest (Waring et al. 2011, Shafer et al. 2015, Turner et al. 2015, 2016). Although these models have characterized important aspects of forest ecology and atmosphere–biosphere dynamics, their simplified representation of species composition and canopy structure may affect their simulation of natural forest stands of the Pacific Northwest in important ways. For example, in Biome-BGC, only one plant functional type (PFT) occupies each site, and no distinct age or size classes are represented (Turner et al. 2015, 2016). 3-PG is a physiologically based stand growth model developed principally for plantation forestry applications but applied widely across the Pacific Northwest (Landsberg and Waring 1997, Waring et al. 2011). 3-PG simulates stem growth and leaf area dynamics of individual species, but it greatly simplifies or does not represent a range of forest processes and characteristics, including respiration, vertical canopy structure, and sub-monthly growth (Waring and McDowell 2002). The Lund-Potsdam-Jena dynamic global vegetation model (LPJ-DGVM; Shafer et al. 2015) captures a suite of biophysical processes but simplifies canopy structure: While multiple PFTs may occupy a site, each PFT is prescribed as only one single average big-leaf. Duarte et al. (2017) evaluated the performance of the Community Land Model version 4.5 (CLM4.5) at Wind River Experimental Forest, but the simulation represents the forest stand as a single needleleaf PFT. Pitfalls of over-simplification of vegetation composition and parameterization in CLM have been recognized by recent studies (Law and Waring 2015), and multiple PFTs with unique physiological parameters are required to represent forest types in the western United States (Buotte et al. 2019). At Wind River site, the old-growth forest has remarkably complex structure, with co-dominant but ecologically distinct conifer species. The potential importance of competition and succession dynamics among the cohorts occupying the multi-layered canopy at Wind River cannot be explored with the above models.

A second-generation dynamic global vegetation model (DGVM; Fisher et al. 2010, 2015, 2018) has the ability to simulate both sub-daily biophysical processes and longer-term demographic processes, thereby enabling exploration of the interaction of the shorter- and longer-term

processes in response to climate drivers. Cohort-based models such as GAPPARD (Scherstjanoi et al. 2014) and TREEMIG (Nabel et al. 2014, Zurbriggen et al. 2014) can better represent the heterogeneity of plants than big-leaf models and have lower computational cost than gap and individual-based models (Dietze and Latimer 2011, Christoffersen et al. 2016, Fischer et al. 2016). In this study, we applied a cohort-based model, the Ecosystem Demography Model 2 (ED2; Medvigy et al. 2009), at the Wind River Experimental Forest, an old-growth forest in Washington with a wealth of observation data and studies (Shaw et al. 2004). ED2 groups plants not only into multiple PFTs, but also into numerous size classes, which enables vertical interactions and resource competitions among different sizes of trees. We assumed that photosynthesis at this mature site was primarily limited by light and water availability (Brooks and Coulombe 2009, Tarvainen et al. 2016, Cornejo-Oviedo et al. 2017) and that variability in observed water and carbon fluxes during the 18-yr study period (1998–2015) was primarily driven by climate. Therefore, we did not simulate nitrogen limitation during this exercise.

Our overall goal was to assess the ability of ED2 to simulate the sub-daily biophysical processes and the stand structure at Wind River, and to conduct an initial exploration of how stand structure interacts with the biophysical processes. In particular, we addressed the following questions:

1. How well can ED2 represent vegetation composition, stand structure, and ecosystem fluxes at Wind River?
2. How do carbon and water fluxes vary among the cohorts that comprise the simulated stand?
3. Are there significant differences in the way the cohorts respond to changes in the observed climate?

By pursuing these questions, we aim to establish the potential utility of using ED2 to explore long-term vegetation response under climate change scenarios (e.g., representative concentration pathways; Van Vuuren et al. 2011), and to lay the foundation for applying a second-generation DGVM across the Pacific Northwest.

Methods

Study site

Wind River Experimental Forest (45.82° N, 121.95° W) is located in the T.T. Munger Research Natural Area, in the southern Cascade Range of Washington State. The forest is situated at 371 m elevation within the relatively flat Wind River Valley on a shallow slope (~3.5%) between two hills, which protect the study area from severe windstorms (Shaw et al. 2004). The soils are generally coarse in texture, well drained, and nutrient poor. Winters are wet and mild with occasional snow, and summers are warm and dry (Falk et al. 2005, 2008). During the period of 1998–2015, the total water-year (October–September) precipitation varied from ~1269 mm to ~2835 mm, with only ~7% falling from June through September. Over the same period, the average annual air temperature varied from 8.1°C to 10.9°C. The winter monthly mean temperature in this period ranged from 0.8°C to 3.6°C, and the summer monthly mean temperature varied between 16.2°C and 20.1°C.

The forest at Wind River has a species composition characteristic of old-growth forests in the Pacific Northwest. It represents the upper boundary of several forest ecosystem gradients in age, biomass, stature, tree density, and structural complexity (Franklin et al. 2002, Suchanek et al. 2004, Falk et al. 2005). The forest is composed of Douglas-fir (*Pseudotsuga menziesii* (Mirb.) Franco), western hemlock (*Tsuga heterophylla* (Raf.) Sarg.), western redcedar (*Thuja plicata* Donn ex D. Don), Pacific yew (*Taxus brevifolia* Nutt.), Pacific silver fir (*Abies amabilis* (Douglas ex Loudon) Douglas ex Forbes), noble fir (*Abies procera* Rehder), grand fir (*Abies grandis* (Douglas ex D. Don) Lindl.), and western white pine (*Pinus monticola* Douglas ex D. Don). The forest has a stand density of 427 trees/ha and basal area of 82.9 m^2/ha. Douglas-fir dominates the forest in basal area (~43%) and wood volume (~50%). However, western hemlock, a late-successional species, comprises the majority of tree stems (~52%) while accounting for 32.4% of the total basal area (Parker et al. 2004, Shaw et al. 2004). Deciduous trees comprise a small component of stand biomass (Thomas and Winner 2000).

The current stand is thought to have originated from a stand-replacing fire approximately 500 yr

ago and has experienced minimal anthropogenic impact since (Shaw et al. 2004). Douglas-fir trees dominate the upper canopy (45–60 m), while western hemlocks dominate the middle canopy (15–45 m), along with occasional western redcedars. Western hemlocks have the greatest foliage area (~53%; Parker et al. 2004). Estimates of one-sided leaf area index (LAI) at the stand range from 6.3 to 9.2, with little seasonality (Parker et al. 2002, Roberts et al. 2004). The vertical distribution of LAI has a bottom-heavy pattern, with the maximum LAI occurring between 15 and 30 m aboveground (Thomas and Winner 2000, Parker et al. 2002). Total carbon storage at the site is estimated at 61.9 kg C/m^2, with 39.8 kg C/m^2 stored in live biomass, 9.6 kg C/m^2 in woody detritus, 9.3 kg C/m^2 in mineral soil, and ~3.2 kg C/m^2 in fine non-woody litter (Harmon et al. 2004).

ED2 model simulation

The ED2 model is a cohort-based terrestrial biosphere model that simulates a comprehensive suite of forest ecosystem processes, including fast-response (half-hourly) biophysical and physiological processes, as well as long-term processes related to changes in forest structure, demography, and biogeochemistry (Medvigy et al. 2009). ED2 represents the landscape as a grid, and within each grid cell, a set of tree cohorts are simulated using partial differential equations to approximate average tree size and density. Species are grouped into plant functional types (PFTs) which are associated with a set of plant physiological traits that govern how a tree interacts with its environment. The default parameterization for the two conifer PFTs in ED2 does not adequately represent the species that currently occur in the Pacific Northwest. Therefore, we used field data to adjust six key PFT-specific parameters and to modify the dbh-to-height allometric functions for the northern pine and the late-successional conifer PFTs, to represent the two dominant tree species, Douglas-fir and western hemlock (Table 1), respectively. A complete list of tree species found at the study site and their associations with the two PFTs are given in Appendix S1: Table S1. The source code for the modified version of ED2 is provided in Data S1.

We ran ED2 for a single grid cell, representing the approximate measurement footprint of the flux tower at the Wind River Canopy Crane Research Facility. As with other ED2 studies (Medvigy and Moorcroft 2012, Trugman et al. 2016), we initialized the simulation using forest inventory data (Shaw et al. 2004). We initialized the simulation with three PFTs: a northern pine PFT representing Douglas-fir, with an initial average diameter at breast height (dbh) of 109.3 cm; a late-successional conifer PFT representing western hemlock, with an initial average dbh of 27.5 cm; and a late-successional broadleaf deciduous tree PFT representing the deciduous species at the site (e.g., vine maple; Appendix S1: Table S1), with an average dbh of 4.8 cm. The initial total soil carbon stock was set to 22.1 kg C/m^2 (Harmon et al. 2004).

Simulations were driven with 1998–2015 half-hourly meteorological and radiation data from Wind River Crane Site (Wharton and Falk 2016), obtained from the AmeriFlux data portal (http://ameriflux.lbl.gov/sites/siteinfo/US-Wrc, Wharton, S. 1998–2016). We spun up the model to stabilize soil moisture values and density-dependent mortality. For the spin-up phase, we used a detrended version of the 1998–2015 meteorological and radiation data, repeating it three times, for a total of 54 simulated years. We assumed that the 18-yr time series was representative of the annual variability of the entire spin-up period.

Model evaluation and analysis

To evaluate the ED2 model skill for predicting stand structure at Wind River, we compared simulated plant densities and tree size distributions of two PFTs with the inventory data. To evaluate how well ED2 can simulate ecosystem dynamics, we compared model outputs against an extensive 18-yr dataset of concurrent observations at Wind River including (1) leaf area index (LAI) stratification within the canopy; (2) sensible and latent heat fluxes; (3) leaf temperature at different canopy heights; (4) soil temperature at 0 cm and 15 cm, and soil moisture at 30 cm and 50 cm; and (5) daily gross primary production (GPP), ecosystem respiration (R_{eco}), net ecosystem production (NEP), and averaged daily heterotrophic respiration (R_H) (Appendix S1: Table S2).

To quantify the variability of carbon and water fluxes among cohorts, we compared GPP among all the cohorts. For comparing stomatal conductance, leaf temperature, and leaf-level VPD, we grouped the cohorts into three thickness-even strata: lower (<20 m), middle (20–40 m), and upper (>40 m) canopies. To examine the

Table 1. Physiological and allometric parameters for northern pine and late-successional conifer plant functional types in ED2 (default parameter values are presented in the parentheses).

Parameter	Unit	ED2	Reference
Northern pines			
Specific leaf area	m^2 leaf/kg C	9.00 (6.0)	Gower (1987), White et al. (2000)
Ratio between fine roots and leaves	kg/kg	0.385 (0.346)	Harmon et al. (2004)
Density-independent mortality rate	yr^{-1}	0.007 (0.003)	Bible (2001)
Turnover rate of leaves	yr^{-1}	0.17 (0.33)	Marshall and Waring (1986)
Turnover rate of fine roots	yr^{-1}	0.26 (0.25)	Turner (1981)
Maximum photosynthesis capacity, T_{air} = 15°C	$\mu mol \cdot CO_2 \cdot m^{-2} \cdot s^{-1}$	15.56 (11.35)	McDowell et al. (2002), Manter et al. (2003)
dbh-to-height allometric parameters (a, b, c), height $= 1.3 + a \times (1 - e^{(-b \times DBH)^c})$	a: meter b, c: none	136.4, 0.003, 0.6965 (27.14, 0.039, 1.0)	Van Pelt and North (1996)
Late-successional conifers			
Specific leaf area	m^2 leaf/kg C	20.66 (10.0)	Hessl et al. (2004)
Ratio between fine roots and leaves	kg/kg	0.385 (0.346)	Harmon et al. (2004)
Density-independent mortality rate	yr^{-1}	0.006 (0.002)	Bible (2001)
Turnover rate of leaves	yr^{-1}	0.17 (0.33)	Marshall and Waring (1986)
Turnover rate of fine roots	yr^{-1}	0.37 (0.26)	White et al. (2000)
Maximum photosynthesis capacity, T_{air} = 15°C	$\mu mol \cdot CO_2 \cdot m^{-2} \cdot s^{-1}$	11.00 (4.54)	McDowell et al. (2002), Manter et al. (2003)
dbh-to-height allometric parameters (a, b, c), height $= 1.3 + a \times (1 - e^{(-b \times DBH)^c})$	a: meter b, c: none	45.0, 0.022, 1.532 (22.79, 0.044, 1.0)	Van Pelt and North (1996)

variability of responses to drought, we compared stomatal conductance, leaf temperature, and VPD of across different heights of canopies between a typical summer (July 2014) and an exceptionally hot and dry summer (July 2015).

To characterize the response of the whole stand to drought, we selected four years with contrasting climates for further examination: a relatively wet and cool year (2012), an exceptionally dry year (2013), a hot year (2014), and an exceptionally hot and dry year (2015). We compared water and carbon fluxes of the four selected years to values from the baseline period of 2002–2011. We examined GPP, NEP, stomatal conductance, evapotranspiration (ET), and soil water content (SWC).

Results

Model–observation comparison

ED2 was able to capture many aspects of PFT composition and canopy structure (Fig. 1). The modeled tree densities for both northern pine (NP) and late-successional conifer (LSC) PFTs agreed well with inventory data for Douglas-fir and western hemlock, respectively (Fig. 1a, b). The modeled slightly underestimated the density of large trees and failed to represent the mid-size ones. The small NP trees are mostly saplings, which have negligible carbon flux and water flux. In terms of tree height, ED2 simulation showed good agreement with measured tree heights of Douglas-fir at the site (Fig. 1c, d). For LSC trees, ED2 slightly underestimated the heights of western hemlock across all size classes. Total LAI (~6.3) simulated by ED2 was close to the value estimated by Parker et al. (2002) using the Beer-Lambert inversion method. However, the simulated vertical distribution of LAI is unlike the observed pattern from Parker et al. (2004), where most leaf biomass is concentrated at heights below 20 m (Fig. 2). This mismatch is primarily due to the fact that ED2 places all the leaves of a given cohort at the height of the cohort. For example, ED2 places all the leaves of a 20 m tall cohort at 20 m height.

ED2 reproduced the observed magnitude, variability, and seasonality of both sensible (H) and latent heat (LE) fluxes measured by an eddy covariance system above the canopy (Fig. 3). Linear regression analysis shows that the modeled daily H and LE have good (R^2 = 0.73) and

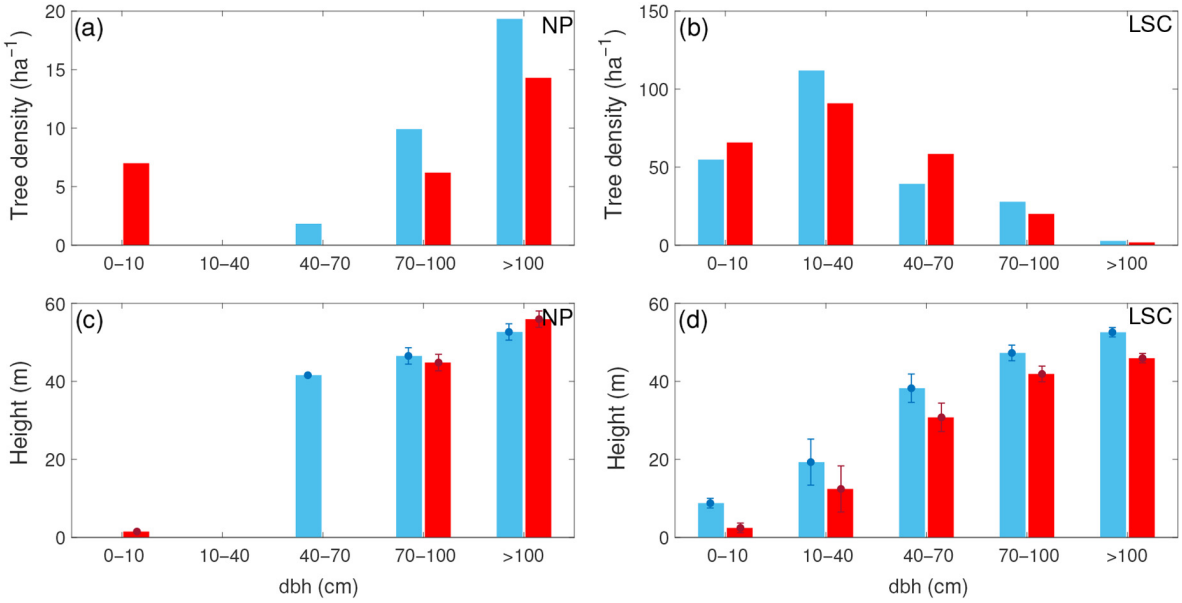

Fig. 1. Modeled and observed tree densities and canopy heights for northern pine and later successional conifer across different dbh sizes.

moderate (R^2 = 0.34) correlation with measured values, respectively. The slopes of regression being less than one indicate overestimations of H and LE by ED2 over the entire study period. The biggest discrepancy between modeled and measured H occurred in 2004, when the model failed to track the substantial canopy-to-atmosphere sensible heat flux observed from late June to early July when the precipitation amount was substantially higher than the other years. Additionally, ED2 and observation agree poorly during some winter days when strong sink of H occurred in the field. We suspect that ice and rain led to erroneous heat flux measurements on those winter days. In most years, the modeled maximum daily LE varied between 80 and 120 W/m^2, except during a few years (1998–2001 and 2006) when ED2 simulated extremely high values. Modeled and observed LE exhibit similar seasonal patterns, especially for the years before 2009. The seasonality of LE flux was variable, with LE becoming a source as early as late April (in 2006) to as late as early August (in 2014). In wet years (2010 and 2012), the modeled LE source was substantially greater than the measurements during the summer. Overall, ED2 slightly overestimated LE flux from the canopy to the atmosphere in spring and summer.

ED2 captured both the magnitude and variability of observed GPP, R_{eco}, and NEP on a seasonal timescale (Fig. 4). On a daily timescale, however, ED2 often underestimated the variability of GPP, R_{eco}, and NEP, compared to the eddy covariance (EC) data. The discrepancies between measured and modeled GPP and R_{eco} did not show a clear seasonal pattern. ED2 poorly models fluxes responding to temperature spikes in the summers of 2006, 2007, and 2013 (Fig. 4). Both modeled and observed daily NEP values ranged between −5 and 5 g C·m^{-2}·d^{-1}. However, ED2 generally fails to capture peak NEP values in the summer. The slope of regression lines with the intercept forced through 0 was close to but slightly less than unity (GPP: 0.92, R_{eco}: 0.90, NEP: 0.95), with relatively high R^2 (GPP: 0.64, R_{eco}: 0.71, NEP: 050) and small RMSE (GPP: 1.31, R_{eco}: 1.05, NEP: 1.21 g C·m^{-2}·d^{-1}; Fig. 4). These lower-than-unity slopes represent a tendency by ED2 to overestimate high flux values (e.g., high NEP in mid-April) and underestimate low flux values (e.g., low GPP in winter).

The 18-yr averaged carbon fluxes from ED2 reproduced the seasonality of the observations, except in the case of simulated R_{eco}, the timing of which appears to precede observations by 1–2 weeks in the spring (Fig. 5a). The averaged

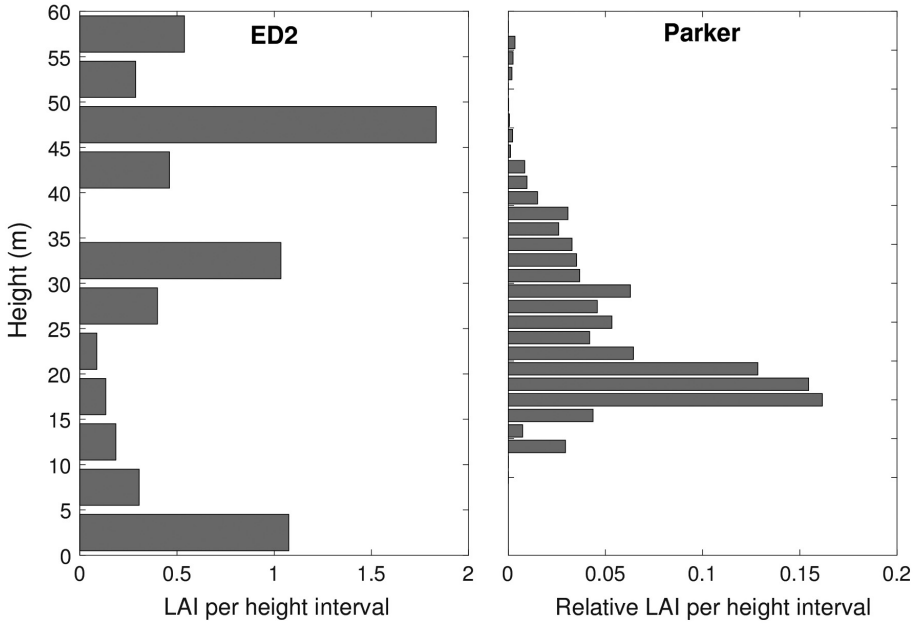

Fig. 2. Modeled and observed vertical distribution of leaf area index (LAI). Since ED2 does not model the vertical distribution of LAI for individual stems or cohorts, simulated LAI is binned according to tree height. Observation data are derived from Parker et al. (2004).

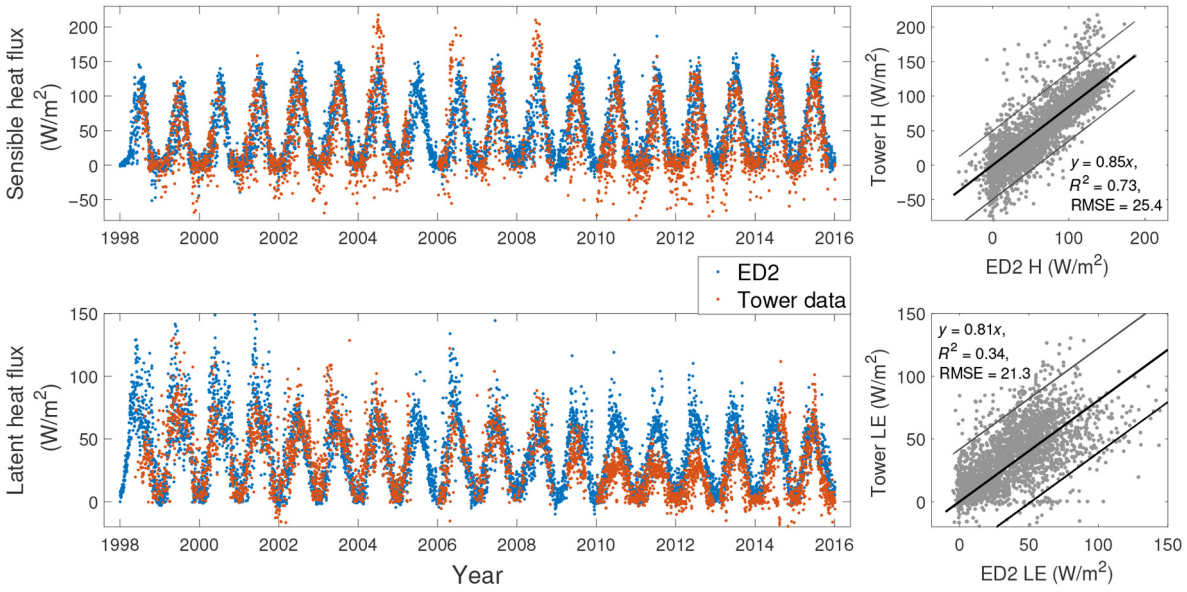

Fig. 3. Comparison of ED2-modeled and measured daily sensible heat flux (W/m^2) and latent heat flux (W/m^2). Positive values denote upward fluxes (i.e., ground to atmosphere). The intercepts of linear fits between model and eddy covariance data are forced to zero. In the right-hand panels, the thick black line represents the regression line, with the 95% confidence interval (thin black lines). In the linear fit for LE, points during 2009–2013 are ignored because of potential sensor calibration error.

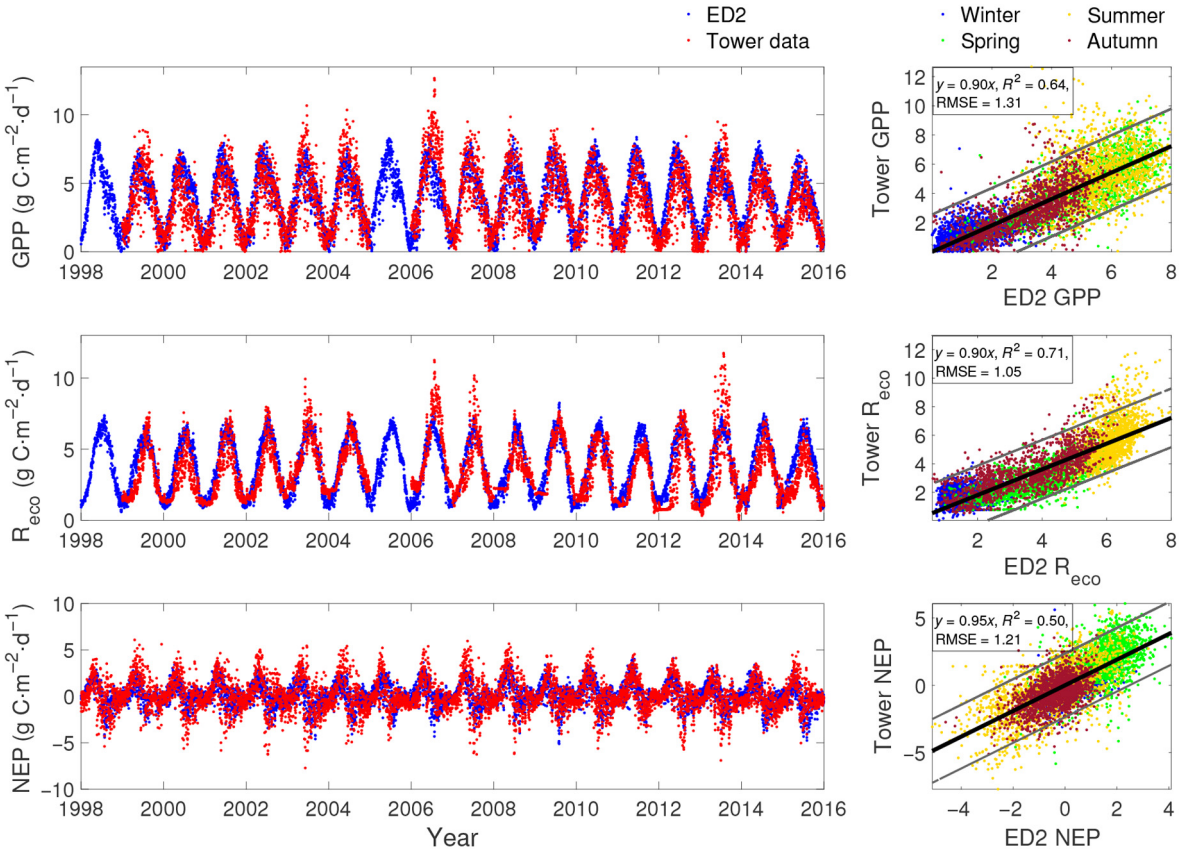

Fig. 4. Comparison of ED2-modeled and data-derived daily GPP, R_{eco}, and NEP, from 1998 to 2015. Here, NEP = −NEE; therefore, positive NEP represents net ecosystem C uptake. The right panels represent linear fittings between modeled and measured fluxes, with intercept forced to zero. In the fitting panels, each season is represented in a unique color: winter (blue), spring (green), summer (orange), and autumn (brown).

peaks in modeled and observed GPP were both about 7 g C·m^{-2}·d^{-1} in mid-June, with slightly lower peak R_{eco} in mid-July. This asymmetric pattern of GPP and R_{eco} resulted in net carbon uptake (i.e., positive NEP) starting from mid-February and ending around late June. The crossover of GPP and R_{eco} occurred around late June; thereafter, the forest was a carbon source until early October when the rainy season started again (Fig. 5b). Therefore, the asymmetry of GPP and R_{eco} determined the net C change throughout a year. This asymmetry is consistent with the eddy covariance-based analysis by Falk et al. (2008). In the spring, ED2 overestimates R_{eco}, resulting in an underestimation of NEP in the spring. Compared with the measured NEP, ED2 slightly underestimated the daily net carbon sink in April by ~0.8 g C·m^{-2}·d^{-1} and overestimated the net carbon source in late July through August by ~0.4 g C·m^{-2}·d^{-1}. Annually, the modeled annual mean GPP (1417.6 ± 51.6 g C·m^{-2}·yr^{-1}) and R_{eco} (1382.3 ± 48.9 g C·m^{-2}·yr^{-1}) summed to 35.3 ± 66.6 g C/m^2 NEP. These estimates are very close to the measured GPP, R_{eco}, and NEP estimates of 1289.2 ± 215.4, 1255.6 ± 216.4, and 26.2 ± 88.1 g C·m^{-2}·yr^{-1}, respectively (Wharton and Falk 2016). In other words, both ED2 and EC data show that the Wind River old-growth forest functioned as a small annual carbon sink during the 18-yr measurement period.

Additionally, ED2 captured the difference between the measured air temperature and top canopy temperature, yet poorly captured the temperature difference between top and bottom canopies (Appendix S1: Fig. S1). The model well reproduced soil temperature and soil moisture

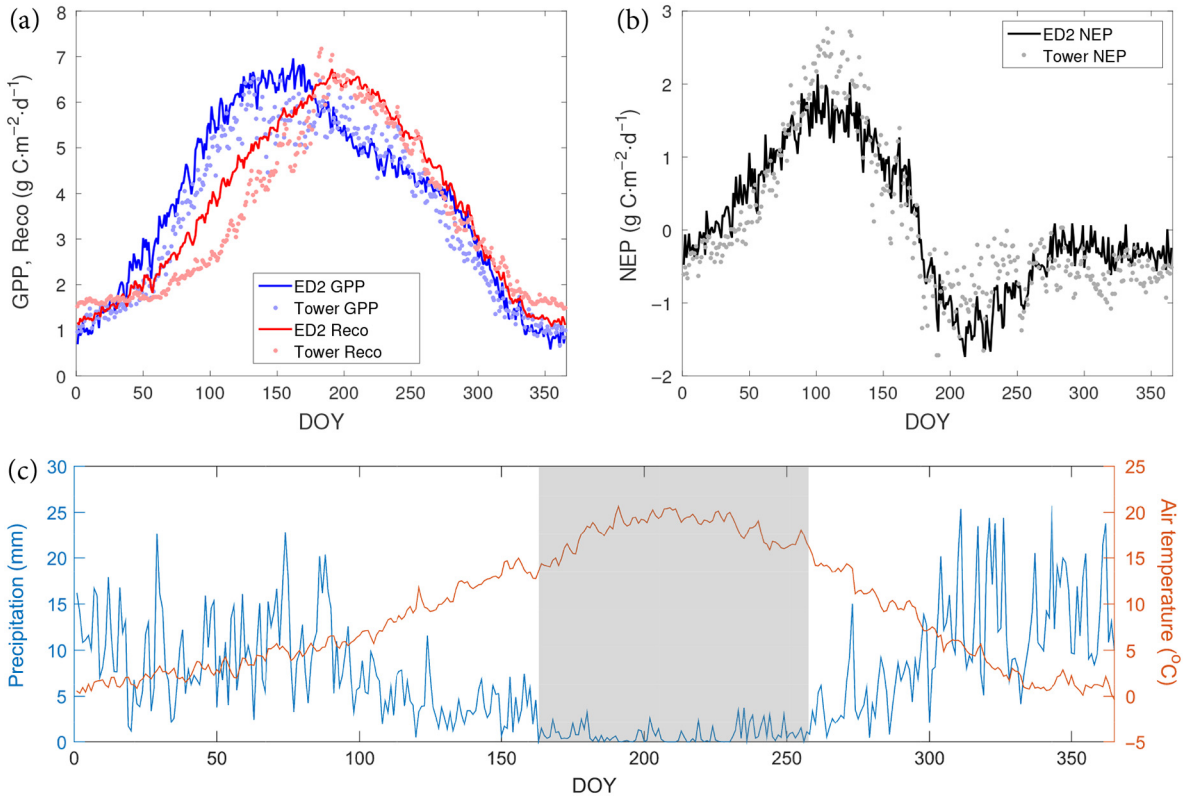

Fig. 5. Comparison of ED2-modeled and data-derived observed daily (a) GPP (g C·m^{-2}·d^{-1}) and R_{eco} (g C·m^{-2}·d^{-1}); (b) NEP (g C m^{-2} d^{-1}); and (c) air temperature and precipitation. The dry season is shaded in (c). All daily time series are averaged from the 18-yr period (1998–2015).

across soil depths (Appendix S1: Figs. S2 and S3). The modeled soil respiration also agreed well with the chamber measurements (Appendix S1: Fig. S4).

Heterogeneity in cohorts

Cohorts simulated by ED2 had distinctly different contributions to carbon fluxes (e.g., GPP; Fig. 6). On an annual basis, tall cohorts (e.g., dbh > 100 cm) accounted for 26% of the total stand GPP. Although the smaller cohorts had much lower GPP, their higher densities still led to the greatest proportion of total GPP. For example, cohorts with dbh < 50 cm contributed 56% of the total stand GPP, and cohorts with dbh between 50 and 100 cm contributed 18%.

Cohorts occupying different heights were sensitive to microclimate. Middle-lower canopy cohorts exhibited stronger responses to warming and drying, when compared to the top canopy (Fig. 7). For example, during a warm and dry July in 2015 ED2 simulated 1.7°C, 0.2°C, and 0.9°C higher leaf temperature and 1.1, 0.4, and 0.7 kPa higher leaf-level VPD (VPD_{leaf}) at lower (<20 m), middle (20–40 m), and upper (>40 m) canopies, respectively, relative to July 2014, a more typical year. Higher leaf temperature with correlated higher leaf-level VPD together led to substantially lower stomatal conductance (gs), especially in middle and lower canopies. Specifically, ED2 predicted on average 0.06, 0.11, and 0.05 mol·m^{-2}·s^{-1} lower gs at lower, middle, and upper canopies, respectively. Stomatal conductance generally increases with cohort height. For example, in July 2014, gs was 0.12 mol·m^{-2}·s^{-1} at 5 m while it was 0.44 mol·m^{-2}·s^{-1} at 60 m. In July 2015, the lower canopy (i.e., <10 m) has relatively high gs (i.e., 0.16 mol·m^{-2}·s^{-1} at 5 m and 0.1 mol·m^{-2}·s^{-1} at 10 m). Between 10 m and

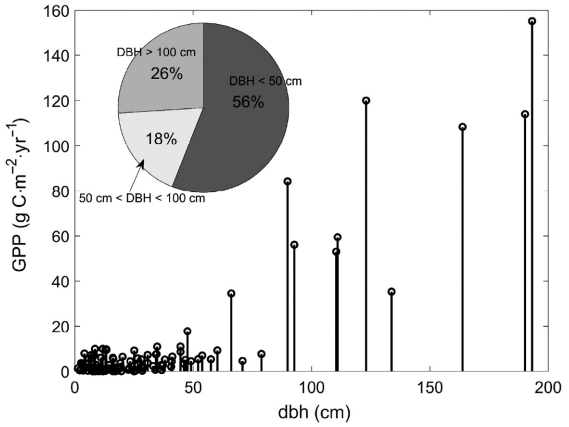

Fig. 6. The ED2-modeled GPP across different size of cohorts. The size of cohorts here is defined by dbh.

60 m, gs increased from 0.04 mol·m^{-2}·s^{-1} to 0.37 mol·m^{-2}·s^{-1}.

The variations in stomatal conductance in responses to drought condition drove distinct changes in GPP across multiple cohorts (Fig. 8). For example, the extreme drought in July 2015 exerted a much stronger effect on the western hemlock occupying the middle-lower canopies (e.g., 10–40 m) than on the Douglas-fir at the upper canopies, reducing the entire stand GPP by about 36%. Although the extreme drought also reduced GPP of Douglas-fir in the upper canopies, the decrease was small relative to the base value.

Ecosystem-level responses to various hydrologic conditions

We compared results from 2012 to 2015, which were droughts years, to results from the baseline period of 2002–2011, to explore ecosystem-level response to drought. Integrating across all cohorts, the ecosystem-level photosynthetic capacity was increasingly sensitive to available water from 2012 to 2015 (Fig. 9). For instance, spring precipitation (March through May) in 2012 was 807 mm higher than the baseline 2002–2011 period, contributing to a 24 g C/m^2 per growing season increase in GPP, despite the average air temperature being ~0.6°C lower than the baseline. In 2014, the warmer (+1.2°C) and wetter (+108 mm) spring also stimulated increased photosynthesis (+13 g C·m^{-2}·season^{-1}), thereby slightly compensating for the reduction in spring net carbon uptake (−15 g C·m^{-2}·season^{-1}) due to enhanced plant and soil respiration. In contrast, 2013 experienced an exceptionally dry (−144 mm) and slightly warmer (+0.7°C) growing season compared to the baseline period, and this led to continuous reduction in GPP from April through August (−24 g C/m^2 per growing season). The growing season of 2015 was even drier and warmer than that of 2013: Spring and summer temperatures were +2.2°C and +2.5°C warmer, respectively, than the baseline period. However, spring and summer precipitation amounts were below baseline averages, which resulted in a substantial reduction in growing season GPP (−133 g C·m^{-2}·growing season^{-1}). The reduction in GPP in 2015, in tandem with a slight increase in ecosystem respiration (34 g C·m^{-2}·growing season^{-1}), led to a net decrease in NEP (−167 g C·m^{-2}·growing season^{-1}) for that year. Because ecosystem respiration was mostly sensitive to air temperature, the warmer growing season exacerbated the drought-induced reductions in NEP in 2013 and 2015 (Fig. 9).

The reduction of carbon uptake in dryer and warmer years was associated with anomalous water fluxes (Fig. 10), which in turn were driven by anomalous VPD and SWC. In 2013 and 2015, elevated VPD from April through August (+0.1 kPa and +0.4 kPa, respectively, relative to the baseline) reduced canopy stomatal conductance by 0.1 and 0.2 g·m^{-2}·s^{-1}, respectively. This reduction was partially responsible for the contemporaneous decrease in GPP (Fig. 9), and contributed to lower evapotranspiration (ET), as seen in year 2015 (−29 kg·m^{-2}·growing season^{-1}). In 2013, reduced stomatal conductance did not lead to a net decrease in ET during the growing season (+7.9 kg·m^{-2}·growing season^{-1}), likely due to higher interception loss of dew from foliar and trunk surfaces, given the modestly higher precipitation in April and May of that year. A similar phenomenon was simulated in 2014: Lower VPD reduced stomatal conductance in April and May, but it did not reduce modeled ET (+4.6 kg·m^{-2}·month^{-1}) because of higher precipitation during those two months (+86 mm). In 2012, VPD was substantially lower than the baseline in June (−0.27 kPa) and July (−0.40 kPa), which drove higher stomatal conductance during those two months (+0.08 and +0.06 g·m^{-2}·s^{-1},

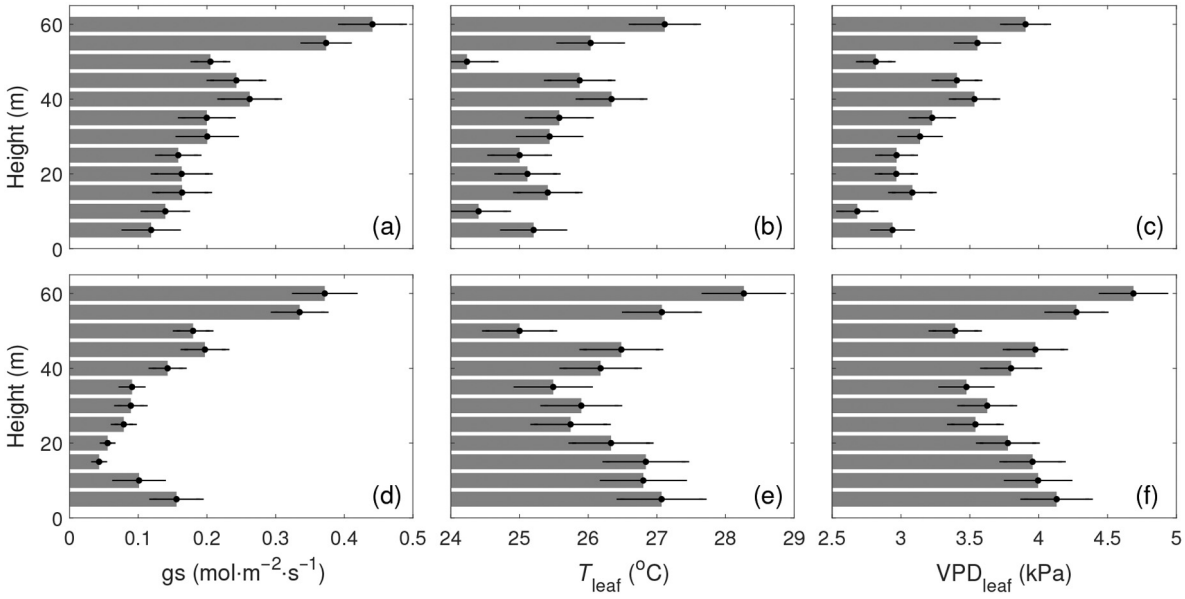

Fig. 7. Modeled stomatal conductance (gs), leaf temperature, and leaf vapor pressure deficit (VPD) across a series of tree height intervals in July 2014 (a–c) and July 2015 (d–f). A specific height does not represent the canopy corresponding to that height, but instead represents tree height.

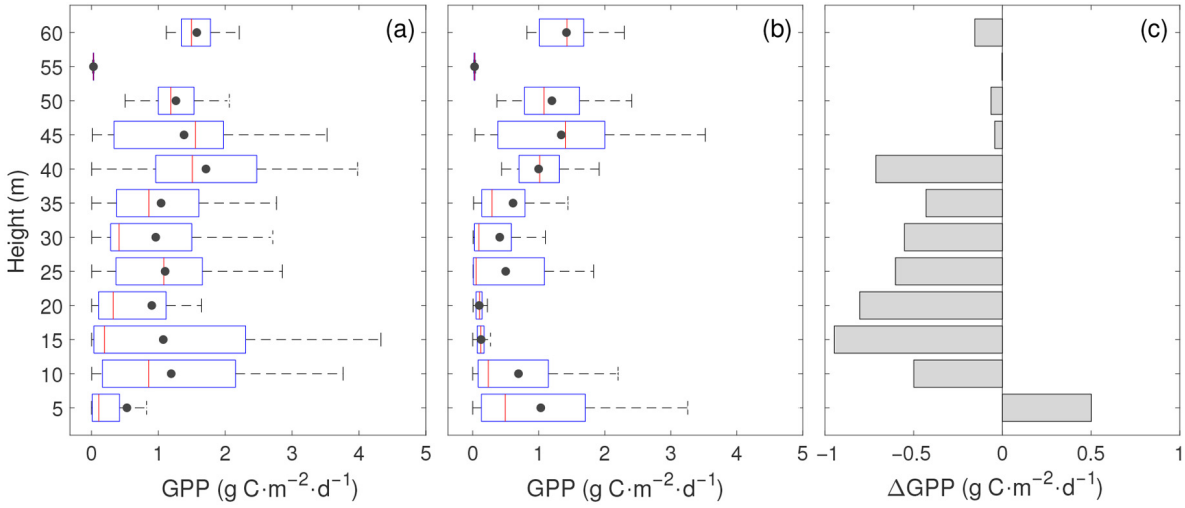

Fig. 8. The ED2-modeled GPP across a series of tree height intervals in (a) July 2014 and (b) July 2015, and (c) the difference of mean GPP between the two years (2015 minus 2014). In (a) and (b), the boxplot with outliers is used to represent all cohorts, and the dark dot represents the mean.

respectively). Among the four years, only 2012 had greater SWC than the baseline for most of the growing season, despite stronger photosynthesis in the summer, because of soil water recharge from an anomalously wet spring. In the other three years, enhanced GPP and ET in early spring did not necessarily reduce SWC in late spring and summer because stomatal conductance was also lower than the baseline. SWC anomalies appear more sensitive to the timing of

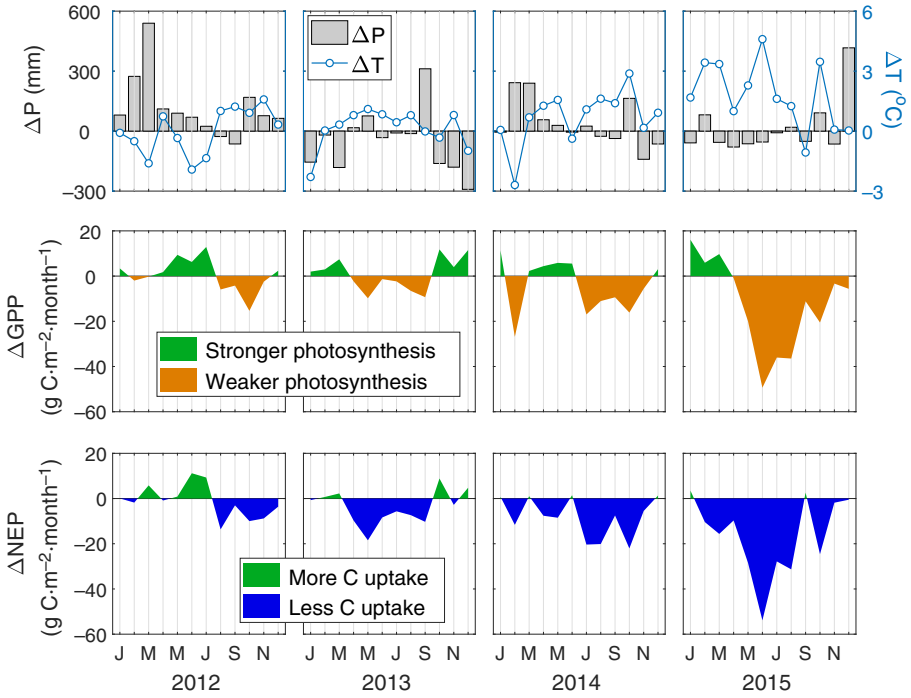

Fig. 9. Anomalies of monthly precipitation, air temperature, GPP, and NEP in 2012, 2013, 2014, and 2015, relative to the baseline period 2002–2011.

precipitation and the variability of air temperature than to ET withdrawals.

During the growing season, stomatal conductance was regulated by both SWC and VPD (Fig. 11a). For this analysis, we calculated the modeled leaf-specific VPD (VPD_{leaf}), since leaf-level measurements emphasize the strong dependence of stomatal conductance on leaf-to-air VPD (Schulze and Hall 1982, Beer et al. 2009). Under low-VPD_{leaf} conditions, stomatal conductance was regulated primarily by SWC, but as VPD_{leaf} increased, the role of SWC diminished, with extreme VPD_{leaf} levels largely shutting down stomatal conductance. For example, on days with midday VPD_{leaf} below 2 kPa, SWC ranged from 0.13 to 0.34 m^3/m^3. In contrast, on days with midday VPD_{leaf} higher than 8 kPa, SWC was limited to the range of 0.15–0.22 m^3/m^3. We illustrate the exceptional levels of drought stress in 2015 by comparing the distribution of midday VPD values for the growing season of 2015 with those taken from the entire 18-yr period (Fig. 11b). The growing season in 2015 was marked by notably more frequent extreme VPD_{leaf} days (>6 kPa) than the entire 18-yr period, which reduced stomatal conductance, ET, and GPP.

Discussion

The unique physiology and longevity of coniferous trees lead to their dominance in the Pacific Northwest (Bible 2001). Broadly generalized parameters for conifers may not work satisfactorily when modeling species in the northwestern United States (White et al. 2000, Hessl et al. 2004). Our use of site-specific parameterization for two coniferous PFTs in ED2 further supports this point. For example, considerably higher SLAs (specific leaf areas) for the two simulated conifers than the default values allow for more biomass allocation to metabolic rather than structural components of leaves. Increasing photosynthetic area per foliage mass of the lower canopy or understory conifer trees effectively increases light-use efficiency (Albani et al. 2006). Consequently, the density-dependent mortality associated with carbon starvation is significantly reduced in the model. Moreover, the other adjusted physiological parameters (Table 1)

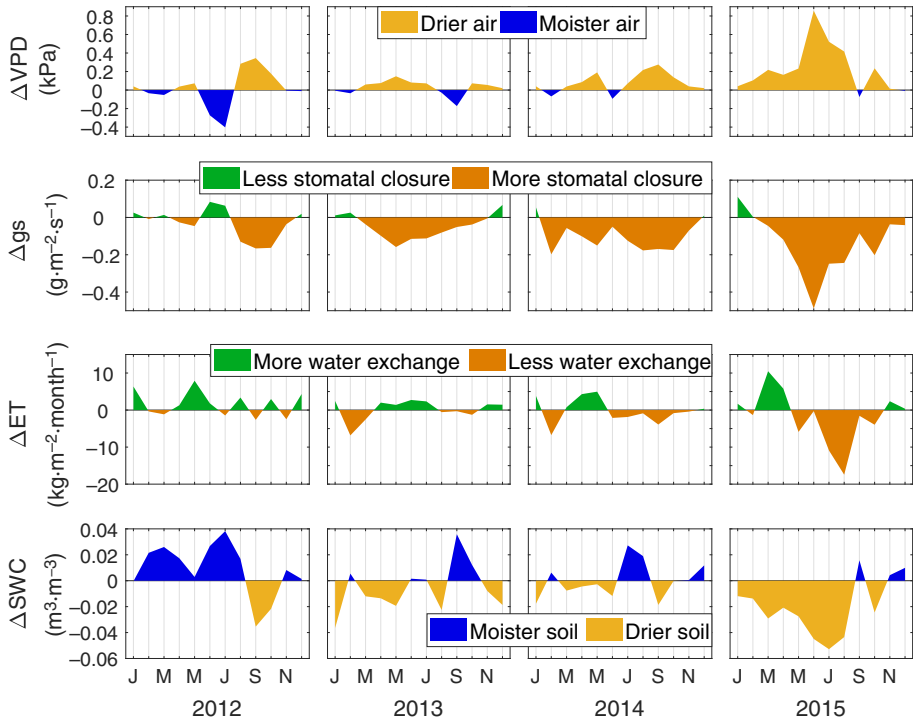

Fig. 10. Anomalies of monthly vapor pressure deficit (VPD), simulated stomatal conductance (gs), evapotranspiration (ET), and soil water content (SWC) in 2012, 2013, 2014, and 2015, relative to the baseline period 2002–2011.

together reduce the carbon cost and increase the productivity of coniferous PFTs, thereby increasing their competitive advantage against temperate deciduous PFTs.

With the improved values for key physiological and allometric parameters, ED2 was able to capture the general patterns of carbon, water, and energy fluxes at the site. The increase in summer stomatal conductance with tree height (Fig. 7) simulated by ED2 is at first puzzling given the opposite phenomenon reported by many (Bond et al. 2007, Woodruff et al. 2009). In the ED2 simulation, the upper-canopy foliage experiences more optimal leaf temperature and received more photosynthetically active radiation (PAR) in the summer than the lower canopy, resulting in higher photosynthetic rates and stomatal conductance. While ED2 may be overestimating the contrast between the upper and lower canopies, it remains possible that in highly shaded stands with sufficient soil moisture, the upper canopy maintains higher levels of productivity than the lower canopy during the summer. The mismatch in leaf skin temperature is partly due to ED2 locating all of a cohort's leaf biomass at a single height. The overestimation of radiative heating within canopy leads to overestimation of autotrophic respiration, which may indicate the model's over-sensitivity to temperature. As a consequence, the simulated R_{eco} increases earlier in the beginning of growing season compared to the observation (Fig. 5).

In the following section, we discuss two primary findings of this study: (1) the importance of representing cohorts at the Wind River old-growth forest, rather than using big-leaf models that represent all the vegetation as a single leaf; and (2) the dynamic mechanisms of response to drought simulated by ED2. Finally, we discussed the limitation in current ED2 and potential effort to improve future simulations.

Importance of representing cohorts

This study highlights the utility of cohort-based models for forest stands with complex structure. Although ED2 does not reproduce spatial distribution of individual trees, representing stand composition and structure in terms of

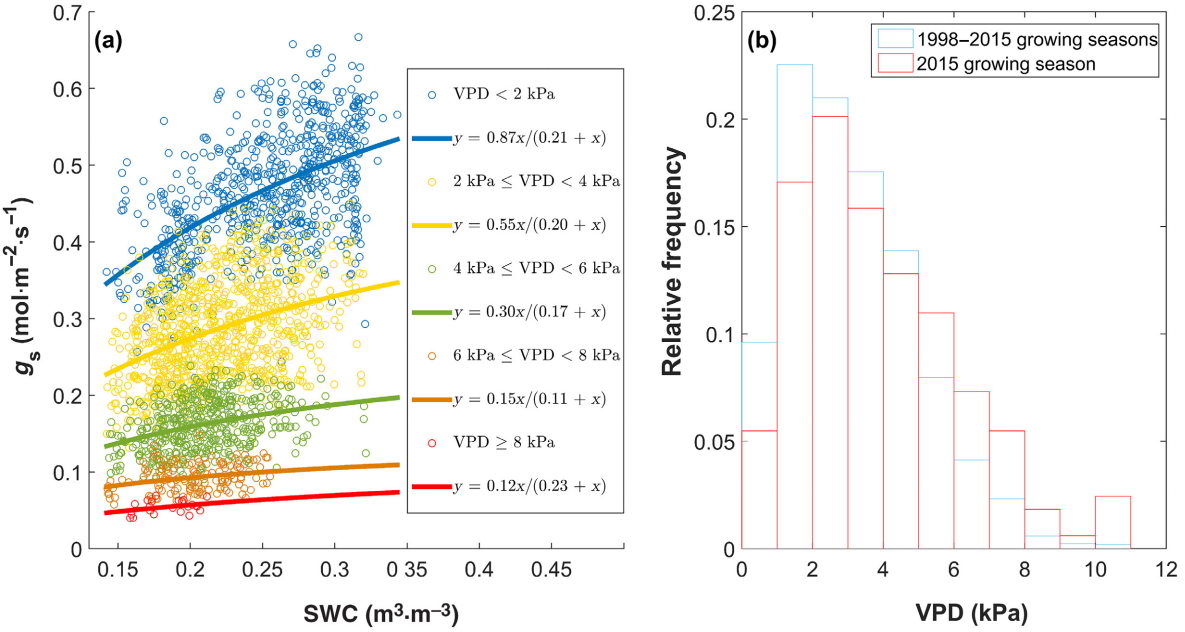

Fig. 11. Stomatal conductance vs. soil water content for intervals of vapor pressure deficit (VPD). (a) Midday (10 a.m.–4 p.m.) stomatal conductance (gs, mol·m^{-2}·s^{-1}) values are plotted against soil water content (SWC, m^3·m^{-3}) across five intervals of VPD, during growing season (April–September) from 1998 to 2015. The solid lines are curves fitted for each VPD interval. SWC represents the top 60 cm soil. (b) The relative frequency of midday VPD for growing season of the 18-yr period (blue) and year 2015 (red). VPD values in (a) and (b) are leaf-specific VPD.

cohorts provides a useful tool to explore and evaluate the non-linear responses of different sizes of trees to climate anomalies. At the Wind River old-growth forest stand, we show that there is a clear divergence of microclimate between top and middle-low canopies. Further, we show that Douglas-fir and western hemlock trees respectively occupy upper and middle-lower canopy layers and respond differently to the stratified microclimate. These results imply that the stand will not respond as a single big-leaf to climate change; instead, the results imply that the canopy layers occupied by different species will respond significantly differently to climate change. In particular, the top canopy, occupied by cohorts of mature Douglas-fir, are less sensitive to drought events, as demonstrated by observed and simulated responses to drought years (e.g., 2015). The large trees are able extract water from deep soil layers (>60 cm) during drought events, where the SWC remains relatively stable even in extremely dry summers (Warren et al. 2005). In contrast, the mid-canopy cohorts (western hemlock) with medium and small sizes of trees can only utilize soil water from shallower layers (<60 cm), where SWC is highly sensitive to atmospheric drying. Although the medium-size western hemlock cohorts have lower stomatal conductance and GPP rates than the large Douglas-fir cohorts, they contribute the most to ecosystem-level fluxes because of their dominance in tree density. This phenomenon is confirmed by our upscaled sap flow data at this site (Rastogi 2018).

A big-leaf ecosystem model can be and have been parameterized to exhibit the ecosystem dynamics at this site for average site conditions and climate. However, we hypothesize that those models will exhibit significant bias under extreme climate events or disturbance. For example, a big-leaf model may overestimate the decline of stomatal conductance and photosynthetic capacity of all trees at the site during drought events, even though mature Douglas-fir is likely to be resilient to a degree of drought. The difference between big-leaf models and cohort-based models will widen as we consider stand response to a rapidly warming climate in

the future. Based on our current modeling results, we hypothesize that previously reported decline of large Douglas-fir trees (Shaw et al. 2005) may underestimate the resilience of Douglas-fir under a rapidly warming climate. Meanwhile, big-leaf models may underestimate the vulnerability of western hemlock that occupy the middle and lower canopies. The resilience of the mature Douglas-fir in the upper canopy may delay succession at the site. The timing of the potential decline of the top canopy (i.e., Douglas-fir >45 m) under a rapidly warming climate, the ecosystem response under the dominance of the new dominant species (i.e., western hemlock), and feedback to the climate (e.g., evapotranspiration and albedo) can be more effectively captured by cohort-based model than big-leaf models.

Dynamic mechanisms of responses to drought

At the ecosystem scale, our simulation indicates that the control of soil moisture on carbon fluxes in the simulation is mainly from the GPP response rather than R_H response, and the Wind River old-growth forest is simulated to be a partially water-limited ecosystem. The ecosystem respiration rate appears moderately resistant to water stress in the summer, and the seasonal reduction in summer soil moisture does not greatly affect the soil decomposition rates (Fig. 5). This is because deeper soil layers retain sufficient moisture, even though the surface soil dries out during summers. Furthermore, the quality of litter and coarse woody debris constrains decomposition rates in the system (Harmon et al. 2011). The abundant overstory leaves and leaf litter at this site help minimize soil water evaporation. Soil respiration rates are modest in the first place because of low organic matter in deeper soil layers, which partly limits the drought-induced change in soil respiration compared to the photosynthetic response.

Temperature control on productivity in the recent past may be a preview of future climate effects (Mariler et al. 2017). The exact effect of a warmer climate on forest productivity will likely depend on the type, timing, and magnitude of future climate anomalies (Sippel et al. 2016). This is illustrated by a comparison of simulation results from two droughts years: 2013 and 2015. Both 2013 and 2015 were exceptionally dry years, receiving low winter and spring precipitation. However, the reduction in GPP was much larger in 2015 than in 2013, because the anomalously warm temperatures in spring 2015 depleted significantly more soil water than in 2013. The enhanced rates of photosynthesis and the depletion of soil water in the early spring further amplified the effect of extreme temperatures later in the summer. In particular, the high temperatures and VPD_{leaf} in summer reduced stomatal conductance far more in 2015 than in 2013. While reductions in GPP are the primary driver of reductions in NEP, reductions in NEP may also reflect ED2's over-sensitivity to temperature for calculating R_{eco} when temperatures warm in the spring. This partly explains the lower NEP in the spring of 2015 than in 2013.

A consistent VPD control on stomatal conductance has been observed both at the stand scale (Sulman et al. 2016) and at multiple biomes across the globe (Novick et al. 2016). Previous studies note that increases in VPD are always detrimental to transpiration and net carbon uptake, regardless of whether there is a co-occurring drought (Eamus et al. 2013). At Wind River, soil water deficit and high VPD do not always coincide. Duarte et al. (2017) applied a process-based model CLM4.5 at the Wind River forest and report that stomatal closure was primarily driven by VPD, rather than by soil moisture. This is likely because CLM4.5 simulates water limitation only in terms of available soil moisture and does not factor in water demand. Therefore, most of the variations in stomatal conductance displayed by CLM4.5 result from the varying effect of VPD on photosynthesis. In contrast, water limitation in ED2 is driven by both supply and demand. In ED2, when VPD is high, demand is low, so soil moisture limitation is low. Thus, drought may reduce stomatal conductance either by simulating stomatal closure at times of high VPD or by reducing available soil moisture. In our simulations, we observe that during periods of low VPD (<2 kPa), stomatal conductance is mainly determined by SWC. However, in exceptionally dry years (e.g., 2015) when VPD_{leaf} is high (>6 kPa), reduction in stomatal conductance was controlled by VPD regardless of soil moisture status. This ability to resolve the different drivers of reductions in stomatal conductance further highlights the utility of ED2 for simulating climate change impacts in moist forests.

Modeling limitation and potential improvement

The multi-layered canopy structure in ED2 allows substantial light penetration into the lower canopy that facilitates light capture by the leaves. However, the use of top-flat scheme where the model locates all leaf biomass of a cohort at the cohort's height, along with the use of Beer-Lambert law for light distribution through the canopy, results in too much radiation penetrating to the lower canopy. As a consequence, lower-canopy leaves receive too much PAR and are heated excessively, which leads to overestimation of photosynthetic rates and underestimation of intercellular carbon dioxide concentrations (ci/ca ratios). A better scheme for vertical distribution of leaf biomass is therefore needed to improve the simulation of the lower canopy and understory physiology of forest ecosystems with complex canopy structures (Weng et al. 2015). Such model improvements are especially important for understanding the growth and demography of shade-tolerant tree species, such as the western hemlock occurring at Wind River.

Although mature stands are able to utilize deep soil water during drought periods, previous studies have found that foliage at the top of tall trees (e.g., height >50 m) often experiences very low water potentials and enhanced likelihood of xylem embolism because of the long transport distance between root layer and upper foliage layer (Ryan and Yoder 1997, Ryan et al. 2006). Not accounting for this long hydraulic pathway may cause overestimation in stomatal conductance in the upper canopy of Douglas-fir at Wind River, which has hydraulic path lengths that exceed 50 m (Wharton et al. 2009). Recent enhancements to ED2 include a mechanistic representation of water-limited photosynthesis, where the model tracks leaf and stem water potential and used it to solve for root zone water uptake, simulate transport of water vertically through the sapwood, and calculate ultimate transpiration rates. The hydrologically enhanced version has been shown to accurately capture ecosystem dynamics at diverse locations around the globe (Trugman et al. 2016, 2018, Xu et al. 2016).

The complex dynamics of forest stand response to drought simulated by ED2—for example, the differences among the cohorts, the different ways that drought reduces net ecosystem productivity, and the importance of high spring temperatures—suggests earlier generations of dynamic vegetation models applied to the region may oversimplify important controls on plant response to climate change. For example, a rule-based biogeography algorithm (Neilson 1995) used in MC1 (Bachelet et al. 2001) and LPJ-DGVM (Sitch et al. 2003) relies on only minimum temperature for survival to rule out deciduous broadleaf trees in the Pacific Northwest (Fisher et al. 2015). However, these rules are built upon the bio-climate relationships diagnosed from historical quasi-steady-state distributions and may not adequately represent the actual mechanisms that may facilitate the establishment or the expansion of deciduous broadleaf species in the Pacific Northwest under a rapidly warming climate. More comprehensive and mechanistic representations of ecosystem dynamics and stand dynamics, such as provided by ED2, may be more instrumental in exploring consequences of climate change on forest succession in the Pacific Northwest.

Conclusions

This study provides a robust model evaluation for the ED2 at an approximately 500-yr-old Douglas-fir–western hemlock forest in the Pacific Northwest, USA. Using site-specific parameterization, the model captures carbon, water, and energy fluxes reported by observation studies and indicates that the old-growth forest was a small carbon sink during the 1998–2015 study period. ED2 simulates multiple cohorts that comprise the stand, and each cohort responds differently to the heterogeneous microclimate throughout the vertical canopy layers. Cohorts of mature Douglas-fir dominate the upper canopy, and by having access to soil water in deep layers, Douglas-fir exhibits greater resilience to drought. Cohorts of western hemlock occupy the understory and, taken together, dominate canopy conductance and productivity at the site. However, western hemlock exhibits greater vulnerability to drought due to its susceptibility to the drying of the shallow soil layers. By disentangling the climatic controls on carbon and water fluxes, our simulations show that precipitation-based drought causes only a modest reduction in forest

productivity. At low and intermediate levels of VPD_{leaf}, stomatal conductance and photosynthesis are controlled primarily by soil moisture. However, during periods of high VPD (>6 kPa), stomata close and conductance and photosynthesis are greatly reduced regardless of soil moisture status. Furthermore, the timing of warm spring temperatures may help deplete soil moisture, setting the stage for more extreme drought effects in the summer. This study emphasizes the utility and the importance of using the next generation of dynamic vegetation model in the Pacific Northwest, a model that has the ability to represent both fast ecosystem processes and the slower processes that govern stand composition and structure. Enhancements to ED2 and further explorations and applications to various sites in the region are expected to provide useful insights into the mechanisms and consequences of forest response to climate change.

Acknowledgments

Yueyang Jiang is supported by a joint-venture agreement 14-JV-11261952-100 between Oregon State University (OSU) and the USDA Forest Service Pacific Northwest Research Station. John B. Kim is supported in part by USDA Forest Service Western Wildland Environmental Threat Assessment Center (WWETAC). Christopher J. Still is supported by a McIntire-Stennis award to OSU.

Literature Cited

Abatzoglou, J. T., and A. P. Williams. 2016. Impact of anthropogenic climate change on wildfire across western US forests. Proceedings of the National Academy of Sciences USA 113:11770–11775.

Albani, M., D. Medvigy, G. C. Hurtt, and P. R. Moorcroft. 2006. The contributions of land-use change, CO_2 fertilization, and climate variability to the Eastern US carbon sink. Global Change Biology 12:2370–2390.

Bachelet, D., J. M. Lenihan, C. Daly, R. P. Neilson, D. S. Ojima and W. J. Parton. 2001. MC1: a dynamic vegetation model for estimating the distribution of vegetation and associated ecosystem fluxes of carbon, nutrients, and water. Pacific Northwest Station General Technical Report PNW-GTR-508.

Beer, C., et al. 2009. Temporal and among-site variability of inherent water use efficiency at the ecosystem level. Global Biogeochemical Cycles 23:1–13.

Bible, K. 2001. Long-term patterns of Douglas-fir and western hemlock mortality in the Cascade Mountains of Oregon and Washington. Dissertation. University of Washington, Seattle, Washington, USA.

Bond, B. J., N. M. Czarnomski, C. Cooper, M. E. Day, and M. S. Greenwood. 2007. Developmental decline in height growth in Douglas-fir. Tree Physiology 27:441–453.

Brooks, J. R., and R. Coulombe. 2009. Physiological responses to fertilization recorded in tree rings: isotopic lessons from a long-term fertilization trial. Ecological Applications 19:1044–1060.

Buotte, P. C., S. Levis, B. E. Law, T. W. Hudiburg, D. E. Rupp, and J. J. Kent. 2019. Near-future forest vulnerability to drought and fire varies across the western United States. Global Change Biology 25:290–303.

Carroll, C., J. R. Dunk, and A. Moilanen. 2010. Optimizing resiliency of reserve networks to climate change: multispecies conservation planning in the Pacific Northwest, USA. Global Change Biology 16:891–904.

Christoffersen, B. O., et al. 2016. Linking hydraulic traits to tropical forest function in a size-structured and trait-driven model (TFS v. 1-Hydro). Geoscientific Model Development 9:4227–4255.

Cornejo-Oviedo, E. H., S. L. Voelker, D. B. Mainwaring, D. A. Maguire, F. C. Meinzer, and J. R. Brooks. 2017. Basal area growth, carbon isotope discrimination, and intrinsic water use efficiency after fertilization of Douglas-fir in the Oregon Coast Range. Forest Ecology and Management 389:285–295.

Davis, R. J., J. L. Ohmann, R. E. Kennedy, W. B. Cohen, M. J. Gregory, Z. Yang, H. M. Roberts, A. N. Gray and T. A. Spies. 2015. Northwest Forest Plan–the first 20 years (1994–2013): status and trends of late-successional and old-growth forests. Gen. Tech. Rep. PNW-GTR-911. U.S. Department of Agriculture, Forest Service, Pacific Northwest Research Station, Portland, Oregon, USA.

Dietze, M. C. and A. M. Latimer. 2011. Forest simulators. Pages 307–316 *in* A. Hastings and L. Gross, editors. Invited chapter in: Sourcebook in theoretical ecology. University of California Press, Berkeley, California, USA.

Duarte, H. F., B. M. Raczka, D. M. Ricciuto, J. C. Lin, C. D. Koven, P. E. Thornton, D. R. Bowling, C. T. Lai, K. J. Bible, and J. R. Ehleringer. 2017. Evaluating the Community Land Model (CLM4.5) at a coniferous forest site in northwestern United States using flux and carbon-isotope measurements. Biogeosciences 14:4315.

Eamus, D., N. Boulain, J. Cleverly, and D. D. Breshears. 2013. Global change-type drought-induced tree

mortality: Vapor pressure deficit is more important than temperature per se in causing decline in tree health. Ecological Evolution 3:2711–2729.

Falk, M., S. Wharton, and M. Schroeder. 2005. Is soil respiration a major contributor to the carbon budget within a Pacific Northwest old-growth forest? Agricultural and Forest Meteorology 135:269–283.

Falk, M., S. Wharton, M. Schroeder, S. Ustin, and K. T. P. U. 2008. Flux partitioning in an old-growth forest: seasonal and interannual dynamics. Tree Physiology 28:509–520.

Field, C. B., and J. Kaduk. 2004. The carbon balance of an old-growth forest: building across approaches. Ecosystems 7:525–533.

Fischer, R., et al. 2016. Lessons learned from applying a forest gap model to understand ecosystem and carbon dynamics of complex tropical forests. Ecological Modelling 326:124–133.

Fisher, R., N. McDowell, D. Purves, P. Moorcroft, S. Sitch, P. Cox, C. Huntingford, P. Meir, and F. I. Woodward. 2010. Assessing uncertainties in a second-generation dynamic vegetation model caused by ecological scale limitations. New Phytologist 187:666–681.

Fisher, R. A., et al. 2015. Taking off the training wheels: the properties of a dynamic vegetation model without climate envelopes, CLM4.5 (ED). Geoscientific Model Development 8:3593–3619.

Fisher, R. A., et al. 2018. Vegetation demographics in Earth System Models: a review of progress and priorities. Global change biology 24:35–54.

Franklin, J. F., K. Cromack, W. Denison, A. McKee, C. Maser, J. Sedell, F. Swanson and G. Juday. 1981. Ecological characteristics of old-growth Douglas-fir forests. USDA Forest Service General Technical Report PNW-118.

Franklin, J. F., and D. S. DeBell. 1988. Thirty-six years of tree population change in an old-growth Pseudotsuga-Tsuga forest. Canadian Journal of Forest Research 18:633–639.

Franklin, J. F. and R. H. Waring. 1980. Distinctive features of the northwestern coniferous forest: development, structure, and function. Forests: fresh perspectives from ecosystem analysis. Oregon State University Press, Corvallis, Oregon, USA.

Franklin, J. F., et al. 2002. Disturbances and structural development of natural forest ecosystems with silvicultural implications, using Douglas-fir forests as an example. Forest Ecology and Management 155:399–423.

Gower, S. T. 1987. A comparison of above-ground productivity and carbon and nutrient allocation patterns of a deciduous (Larix occidentalis) and an evergreen (Pinus contorta) conifer in the east slopes of the Washington Cascades. Dissertation 34825, University of Washington, Seattle, Washington, USA.

Harmon, M. E., K. Bible, M. G. Ryan, D. C. Shaw, H. Chen, J. Klopatek, and X. Li. 2004. Production, respiration, and overall carbon balance in an old-growth Pseudotsuga-Tsuga forest ecosystem. Ecosystems 7:498–512.

Harmon, M. E., B. Bond-Lamberty, J. Tang, and R. Vargas. 2011. Heterotrophic respiration in disturbed forests: a review with examples from North America. Journal of Geophysical Research: Biogeosciences 116:1–17.

Hessl, A. E., C. Milesi, M. A. White, D. L. Peterson, and R. E. Keane. 2004. Ecophysiological parameters for Pacific Northwest trees. Rep. PNW-GTR-618. U.S. Dep. of Agric., For. Serv., Pacific Northwest Res. Stn., Portland, Oregon, USA.

Hudiburg, T. W., B. E. Law, D. P. Turner, J. Campbell, D. Donato, and M. Duane. 2009. Carbon dynamics of Oregon and Northern California forests and potential land-based carbon storage. Ecological Applications 19:163–180.

Kim, J. B., B. G. Marcot, D. H. Olson, B. Van Horne, J. A. Vano, M. S. Hand, L. A. Salas, M. J. Case, P. E. Hennon, and D. V. D'Amore. 2017. Climate-smart approaches to managing forests. Pages 225–242 *in* D. H. Olson, and B. Van Horne, editors. People, forests, and change. Island Press, Washington, D.C., USA.

Landsberg, J. J., and R. H. Waring. 1997. A generalized model of forest productivity using simplified concepts of radiation-use efficiency, carbon balance and partitioning. Forest Ecology and Management 95:209–228.

Latta, G., H. Temesgen, D. Adams, and T. Barrett. 2010. Analysis of potential impacts of climate change on forests of the United States Pacific Northwest. Forest Ecology and Management 259:720–729.

Law, B. E., and R. H. Waring. 2015. Carbon implications of current and future effects of drought, fire and management on Pacific Northwest forests. Forest Ecology and Management 355:4–14.

Littell, J. S., E. E. Oneil, D. McKenzie, J. A. Hicke, J. A. Lutz, R. A. Norheim, and M. M. Elsner. 2010. Forest ecosystems, disturbance, and climatic change in Washington State, USA. Climatic change 102:129–158.

Manter, D. K., B. J. Bond, K. L. Kavanagh, J. K. Stone, and G. M. Filip. 2003. Modelling the impacts of the foliar pathogen, Phaeocryptopus gaeumannii, on Douglas-fir physiology: net canopy carbon assimilation, needle abscission and growth. Ecological Modelling 164:211–226.

Mariler, M. E., M. Xiao, R. Engel, B. Livneh, J. Abatzoglou, and D. P. Lettenmaier. 2017. The 2015

drought in Washington State: A harbinger of things to come? Environmental Research Letters 12: 114008.

Marshall, J. D., and R. H. Waring. 1986. Comparison of methods of estimating leaf-area index in old-growth Douglas-fir. Ecology 67:975–979.

McDowell, N. G., N. Phillips, C. Lunch, B. J. Bond, and M. G. Ryan. 2002. An investigation of hydraulic limitation and compensation in large, old Douglas-fir trees. Tree Physiology 22:763–774.

Medvigy, D., and P. R. Moorcroft. 2012. Regional scale prediction of forest dynamics: evaluation of a terrestrial biosphere model for northeastern U.S. forests. Philosophical Transactions of the Royal Society B 367:222–235.

Medvigy, D., S. C. Wofsy, J. W. Munger, D. Y. Hollinger, and P. R. Moorcroft. 2009. Mechanistic scaling of ecosystem function and dynamics in space and time: Ecosystem Demography model version 2. Journal of Geophysical Research 114:G01002.

Nabel, J. E., J. W. Kirchner, N. Zurbriggen, F. Kienast, and H. Lischke. 2014. Extrapolation methods for climate time series revisited–Spatial correlations in climatic fluctuations influence simulated tree species abundance and migration. Ecological Complexity 20:315–324.

Neilson, R. P. 1995. A model for predicting continental-scale vegetation distribution and water balance. Ecological Applications 5:362–385.

Novick, K. A., et al. 2016. The increasing importance of atmospheric demand for ecosystem water and carbon fluxes. Nature climate change 6:1023–1027.

Parker, G. G., M. M. Davis, and S. M. Chapotin. 2002. Canopy light transmittance in Douglas-fir/western hemlock stands. Tree Physiology 22:147–157.

Parker, G. G., M. E. Harmon, M. A. Lefsky, J. Chen, R. Van Pelt, S. B. Weis, S. C. Thomas, W. E. Winner, D. C. Shaw, and J. F. Frankling. 2004. Three-dimensional structure of an old-growth Pseudotsuga-Tsuga canopy and its implications for radiation balance, microclimate, and gas exchange. Ecosystems 7:440–453.

Paw U, K. T., et al. 2004. Carbon dioxide exchange between an old-growth forest and the atmosphere. Ecosystems 7:513–524.

Rastogi, B. 2018. Ecosystem Photosynthesis and Forest-Atmosphere Interactions Inferred from Carbonyl Sulfide. Dissertation. Oregon State University, Corvallis, Oregon, USA.

Riley, K. L., and R. A. Loehman. 2016. Mid-21st-century climate changes increase predicted fire occurrence and fire season length, Northern Rocky Mountains, United States. Ecosphere 7:e01543.

Roberts, D. A., S. L. Ustin, S. Ogunjemiyo, J. Greenberg, S. Z. Dobrowski, J. Chen, and T. M. Hinckley. 2004. Spectral and structural measures of Northwest forest vegetation at leaf to landscape scales. Ecosystems 7:545–562.

Ryan, M. G., N. Phillips, and B. J. Bond. 2006. The hydraulic limitation hypothesis revisited. Plant, Cell & Environment 29:367–381.

Ryan, M. G., and B. J. Yoder. 1997. Hydraulic limits to tree height and tree growth. BioScience 47:235–242.

Scherstjanoi, M., J. O. Kaplan, and H. Lischke. 2014. Application of a computationally efficient method to approximate gap model results with a probabilistic approach. Geoscientific Model Development 7:1543–1571.

Schimel, D., et al. 2000. Contribution of increasing CO_2 and climate to carbon storage by ecosystems in the United States. Science 287:2004–2006.

Schulze, E.-D., and A. E. Hall. 1982. Stomatal responses and water loss and CO_2 assimilation rates of plants in contrasting environments, in Encyclopedia of Plant Physiology. Volume 12B. Water Relations and Photosynthetic Productivity, Springer, Berlin, Germany.

Shafer, S. L., P. J. Bartlein, E. M. Gray, and R. T. Pelltier. 2015. Projected Future Vegetation Changes for the Northwest United States and Southwest Canada at a Fine Spatial Resolution Using a Dynamic Global Vegetation Model. PLoS ONE 10:e0138759.

Shaw, D. C., J. Chen, E. A. Freeman, and D. M. Braun. 2005. Spatial and population characteristics of dwarf mistletoe infected trees in an old-growth Douglas-fir western hemlock forest. Canadian Journal of Forest Research 35:990–1001.

Shaw, D. C., J. F. Franklin, K. Bible, J. Klopatek, E. Freeman, S. Greene, and G. G. Parker. 2004. Ecological setting of the Wind River old-growth forest. Ecosystems 7:427–439.

Sippel, S., J. Zscheischler, and M. Reichstein. 2016. Ecosystem impacts of climate extremes crucially depend on the timing. Proceedings of the National Academy of Sciences USA 113:5768–5770.

Sitch, S., et al. 2003. Evaluation of ecosystem dynamics, plant geography and terrestrial carbon cycling in the LPJ dynamic global vegetation model. Global Change Biology 9:161–185.

Smithwick, E. A. H., M. E. Harmon, S. M. Remillard, S. A. Acker, and J. F. Franklin. 2002. Potential upper bounds of carbon stores in forests of the Pacific Northwest. Ecological Applications 12:1303–1317.

Spies, T. A., T. W. Giesen, F. J. Swanson, J. F. Franklin, D. Lach, and K. N. Johnson. 2010. Climate change adaptation strategies for federal forests of the Pacific Northwest, USA: ecological, policy, and socio-economic perspectives. Landscape Ecology 25:1185–1199.

Suchanek, T. H., H. A. Mooney, J. F. Franklin, H. Gucinski, and S. L. Ustin. 2004. Carbon dynamics of an old-growth forest. Ecosystems 7:421–426.

Sulman, B. N., D. T. Roman, K. Yi, L. Wang, R. P. Phillips, and K. A. Novick. 2016. High atmospheric demand for water can limit forest carbon uptake and transpiration as severely as dry soil. Geophysical Research Letters 43:9686–9695.

Tarvainen, L., M. Lutz, M. Räntfors, T. Näsholm, and G. Wallin. 2016. Increased needle nitrogen contents did not improve shoot photosynthetic performance of mature nitrogen-poor Scots pine trees. Frontiers in Plant Science 7:1051.

Thomas, S. C., and W. E. Winner. 2000. Leaf area index of an old-growth Douglas-fir forest estimated from direct structural measurements in the canopy. Canadian Journal of Forest Research 30: 1922–1930.

Trugman, A. T., N. J. Fenton, Y. Bergeron, X. Xu, L. R. Welp, and D. Medvigy. 2016. Climate, soil organic layer, and nitrogen jointly drive forest development after fire in the North American boreal zone. Journal of Advances in Modeling Earth Systems 8:1180–1209.

Trugman, A. T., D. Medvigy, W. Hoffmann, and A. F. A. Pellegrini. 2018. Sensitivity of woody carbon stocks to bark investment strategy in Neotropical savannas and forests. Biogeosciences 15:233–243.

Turner, J. 1981. Nutrient cycling in an age sequence of western Washington Douglas-fir stands. Annals of Botany 48:159–169.

Turner, D. P., W. D. Ritts, R. E. Kennedy, A. N. Gray, and Z. Yang. 2015. Effects of harvest, fire, and pest/pathogen disturbances on the West Cascades ecoregion carbon balance. Carbon Balance and Management 10:12.

Turner, D. P., W. D. Ritts, R. E. Kennedy, A. N. Gray, and Z. Yang. 2016. Regional carbon cycle responses to 25 years of variation in climate and disturbance in the US Pacific Northwest. Regional Environmental Change 16:2345–2355.

Van Pelt, R., and M. P. North. 1996. Analyzing canopy structure in Pacific Northwest old-growth forests with a stand-scale crown model. Northwest Science 70:15–30.

Van Vuuren, D. P., et al. 2011. The representative concentration pathways: an overview. Climatic Change 109:5.

Waring, R. H., N. C. Coops, and S. W. Running. 2011. Predicting satellite-derived patterns of large-scale disturbances in forests of the Pacific Northwest Region in response to recent climatic variation. Remote Sensing of Environment 115:3554–3566.

Waring, R. H., and N. McDowell. 2002. Use of a physiological process model with forestry yield tables to set limits on annual carbon balances. Tree Physiology 22:179–188.

Warren, J. M., F. C. Meinzer, J. R. Brooks, and J. C. Domec. 2005. Vertical stratification of soil water storage and release dynamics in Pacific Northwest coniferous forests. Agricultural and Forest Meteorology 130:39–58.

Weng, E. S., S. Malyshev, J. W. Lichstein, C. E. Farrior, R. Dybzinski, T. Zhang, E. Shevliakova, and S. W. Pacala. 2015. Scaling from individual trees to forests in an Earth system modeling framework using a mathematically tractable model of height-structured competition. Biogeosciences 12:2655–2694.

Wharton, S., and M. Falk. 2016. Climate indices strongly influence old-growth forest carbon exchange. Environmental Research Letters 11:044016.

Wharton, S., M. Schroeder, K. Bible, and M. Falk. 2009. Stand-level gas-exchange responses to seasonal drought in very young versus old Douglas-fir forests of the Pacific Northwest, USA. Tree Physiology 29:959–974.

White, M. A., P. E. Thornton, S. W. Running, and R. R. Nemani. 2000. Parameterization and sensitivity analysis of the BIOME–BGC terrestrial ecosystem model: net primary production controls. Earth Interactions 4:1–85.

Woodruff, D. R., F. C. Meinzer, B. Lachenbruch, and D. M. Johnson. 2009. Coordination of leaf structure and gas exchange along a height gradient in a tall conifer. Tree Physiology 29:261–272.

Xu, X., D. Medvigy, J. S. Powers, J. M. Becknell, and K. Guan. 2016. Diversity in plant hydraulic traits explains seasonal and inter-annual variations of vegetation dynamics in seasonally dry tropical forests. New Phytologist 212:80–95.

Zurbriggen, N., J. Nabel, M. Teich, P. Bebi, and H. Lischke. 2014. Explicit avalanche-forest feedback simulations improve the performance of a coupled avalanche-forest model. Ecological Complexity 17:56–66.

Supporting Information

Additional Supporting Information may be found online at: http://onlinelibrary.wiley.com/doi/10.1002/ecs2.2692/full